Table 2.5 Solar system data: mass characteristics and orbit

Object	Mass (10^{24} kg)	$R_{equator}$(m) Equatorial radius	Density (10^3 kg/m^3)	Angular momentum (10^{39} kg m^2/s)	Average speed (km/s)	a(AU) Semi-major axis of orbit[2]	e Orbital eccentricity	i (°) Orbital inclination[3]	Sidereal period (years)
Sun	1.99×10^6	0.696×10^9	1.409	170[1]	—	—	—	—	—
Mercury	0.33	2.44×10^6	5.46	0.906	47.9	0.3871	0.206	7.00	0.241
Venus	4.87	6.05×10^6	5.23	18.5	35.1	0.7233	0.007	3.39	0.615
Earth	5.97	6.38×10^6	5.52	26.7	29.8	1.0000	0.017	0.00	1.000
Mars	0.642	3.40×10^6	3.92	3.52	24.2	1.5237	0.093	1.85	1.881
Jupiter	1899	7.15×10^7	1.31	19 400	13.1	5.2028	0.048	1.31	11.862
Saturn	568	6.03×10^7	0.7	7840	9.64	9.5388	0.056	2.49	29.46
Uranus	87.2	2.56×10^7	1.3	1700	6.81	19.1914	0.046	0.77	84.01
Neptune	102	2.48×10^7	4.66	2500	5.44	30.0611	0.010	1.77	164.79
Pluto	0.66	1.20×10^6	4.9	17.9	4.75	39.5294	0.248	17.15	248.43

[1] Spin angular momentum of the Sun.
[2] 1 AU = 1.496×10^{11} m.
[3] Inclination of orbit plane relative to the ecliptic.
See also Tables 2.6, 2.7 and 4.1.

Table 4.1 · Some physical properties of the major bodies in the solar system, including Earth's Moon. See also Tables 2.5, 2.6 and 2.7 of Chapter 2. The sphere of influence (see Section 5.8.1 of Chapter 5) is expressed with respect to the Sun as the disturbing body

Parameter\ Body	μ (m^3/s^2) Gravitational parameter	Equatorial surface gravity (m/s^2)	Surface escape velocity (m/s)	Oblateness J_2	Sphere of influence (10^6 km)	Axial rotation period (sidereal)
Sun	1.327×10^{20}	273.98	6.18×10^5	—	—	~ 27 days
Mercury	2.203×10^{13}	3.70	4250	—	0.09–0.14	58.646 days
Venus	3.249×10^{14}	8.87	10 360	2.7×10^{-5}	0.61–0.62	243.019 days
Earth	3.986×10^{14}	9.81	11 180	0.001083	0.91–0.94	$23^h 56^m 22.7^s$
Mars	4.283×10^{13}	3.71	5020	0.001964	0.52–0.63	$24^h 37^m 22.6^s$
Jupiter	1.267×10^{17}	23.12	59 530	0.01475	45.9–50.5	$\sim 9^h 50^m$
Saturn	3.794×10^{16}	9.05	35 560	0.01645	51.6–57.5	$\sim 10^h 15^m$
Uranus	5.780×10^{15}	7.77	21 250	0.012	49.4–54.1	$\sim 17^h 50^m$
Neptune	6.871×10^{15}	11.00	23 540	0.004	85.7–87.6	$\sim 19^h 10^m$
Pluto	1.021×10^{12}	0.40	1300	—	11.4–18.8	6.387 days
Moon	4.903×10^{12}	1.62	2380	0.0002027	0.157–0.162	27.322 days

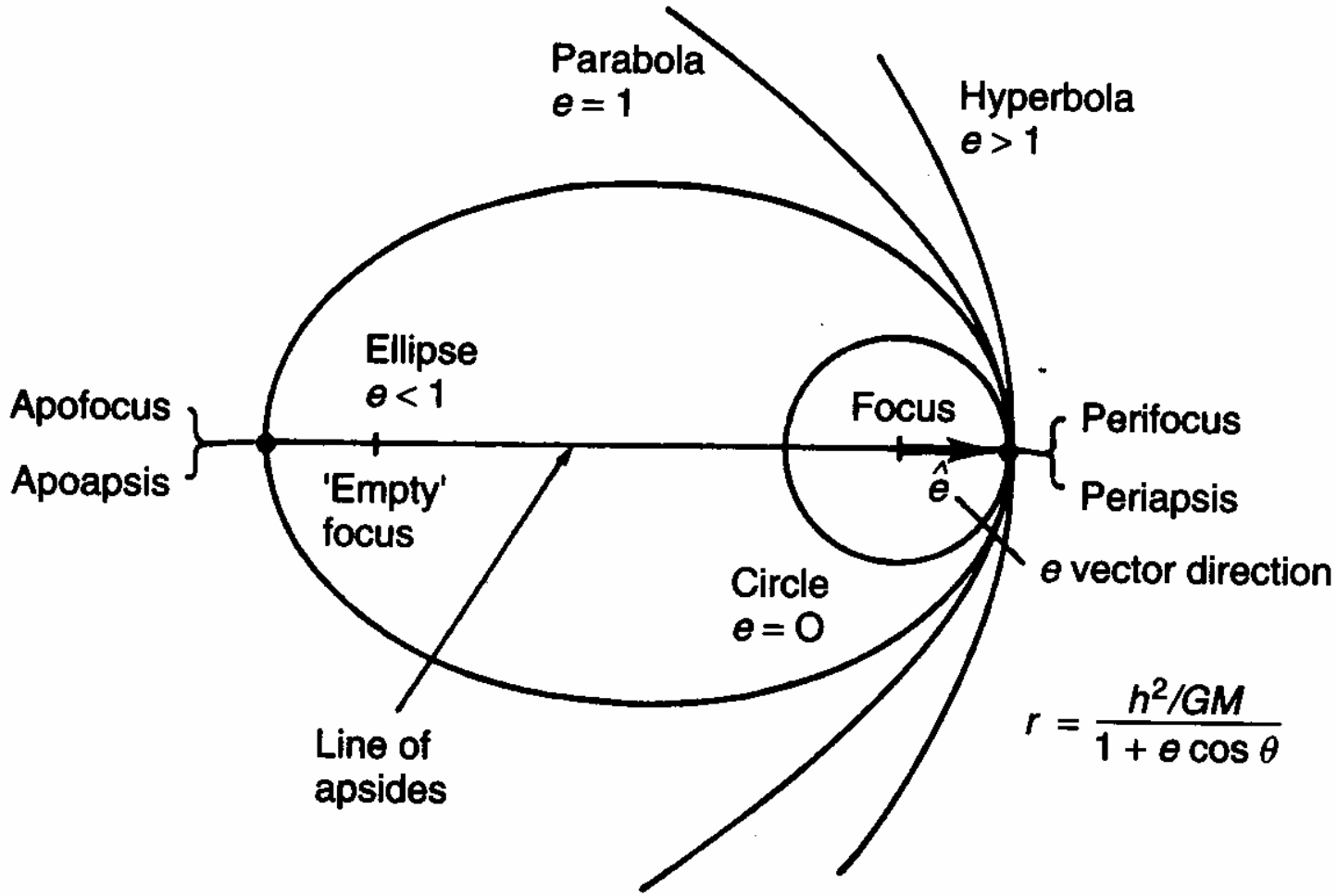

Figure 4.4 Conic sections

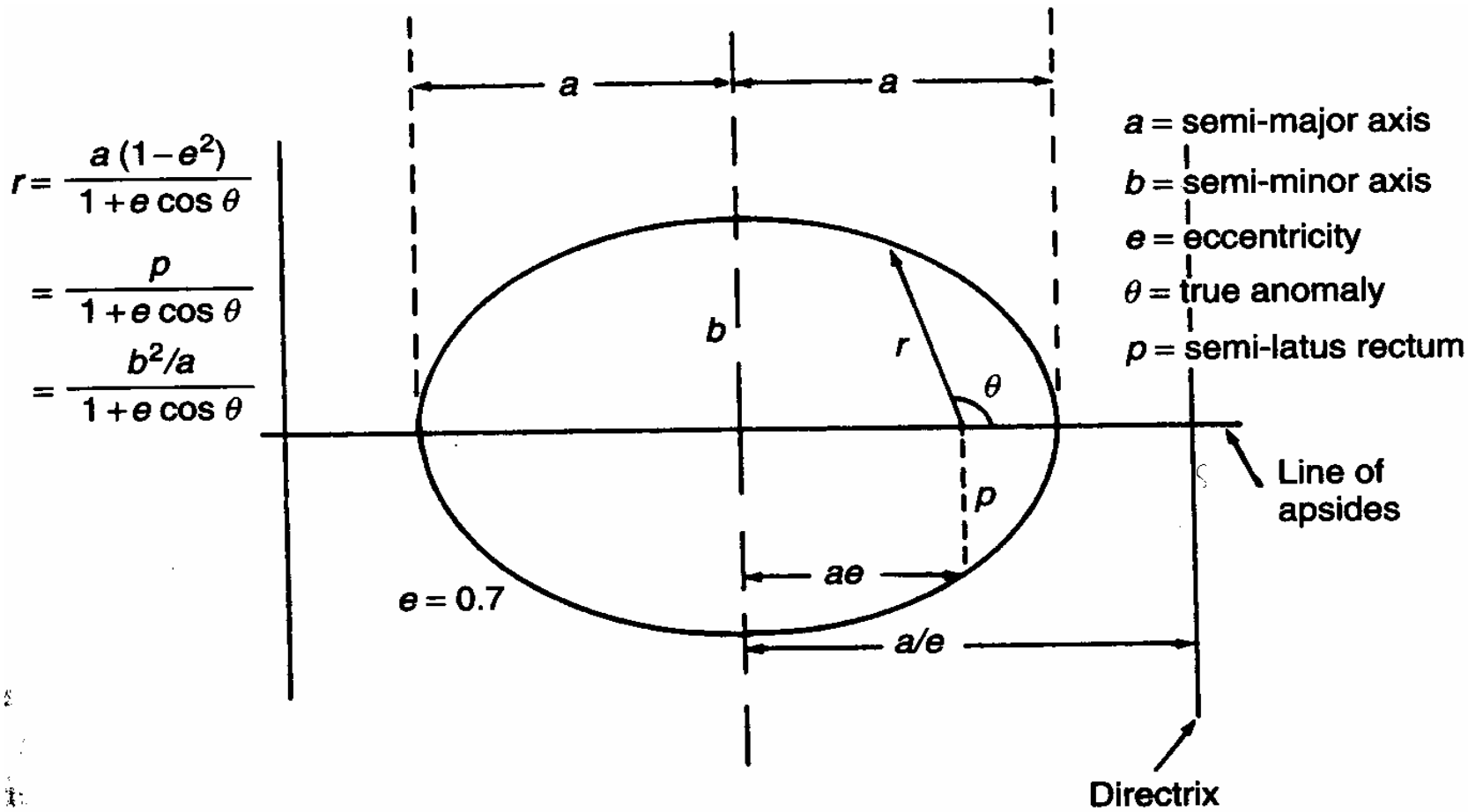

Figure 4.5 Ellipses

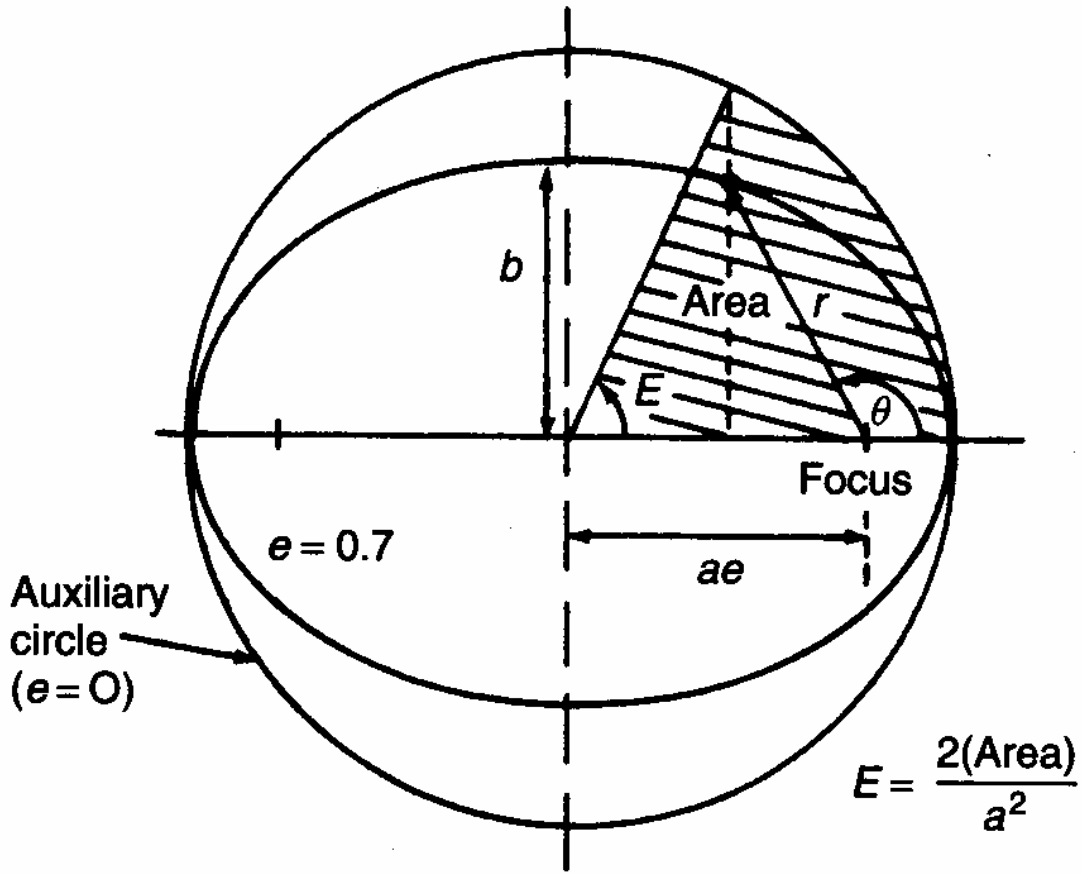

Figure 4.6 Eccentric anomaly definition

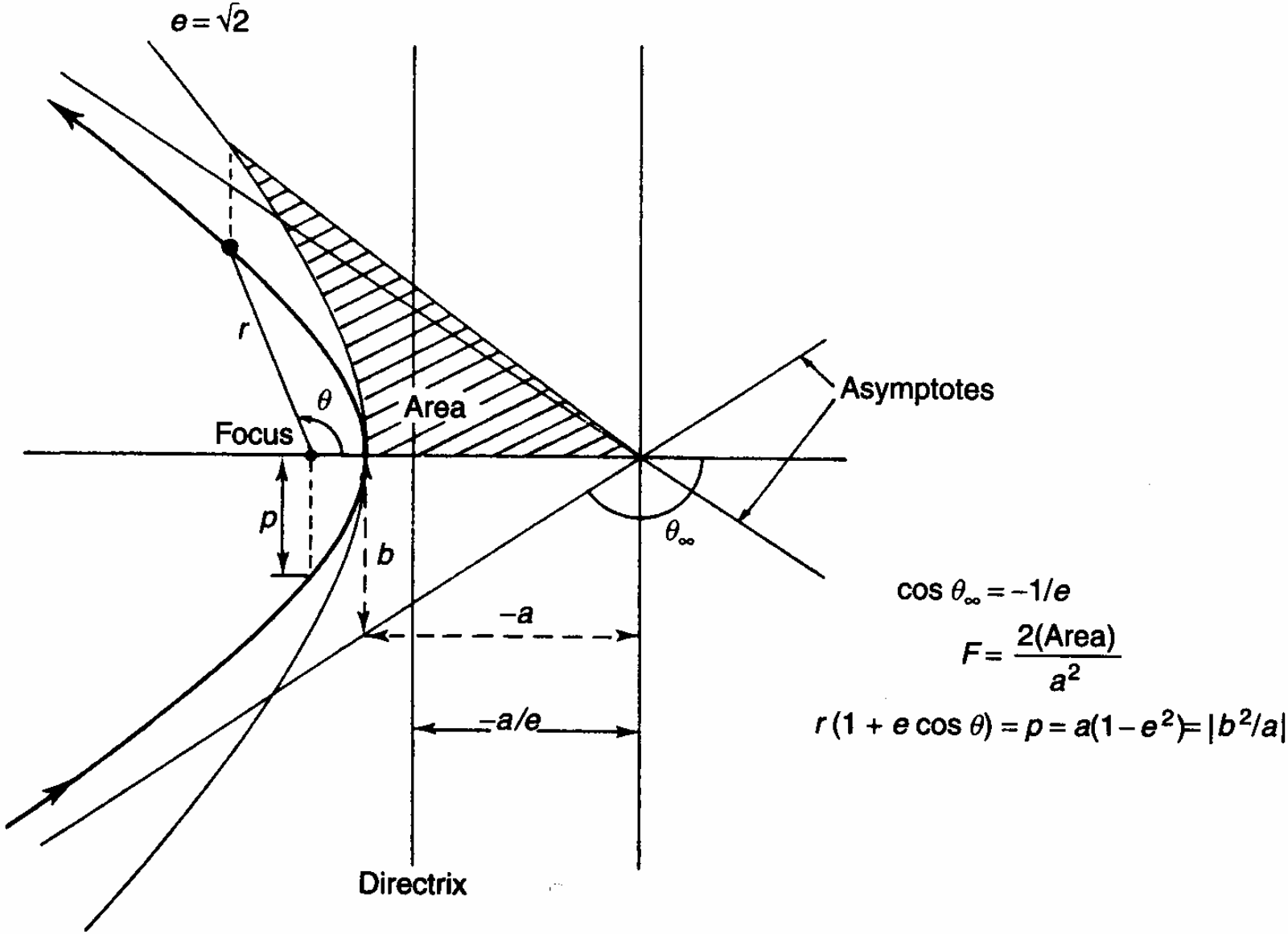

Figure 4.8 Hyperbola ($e > 1$)

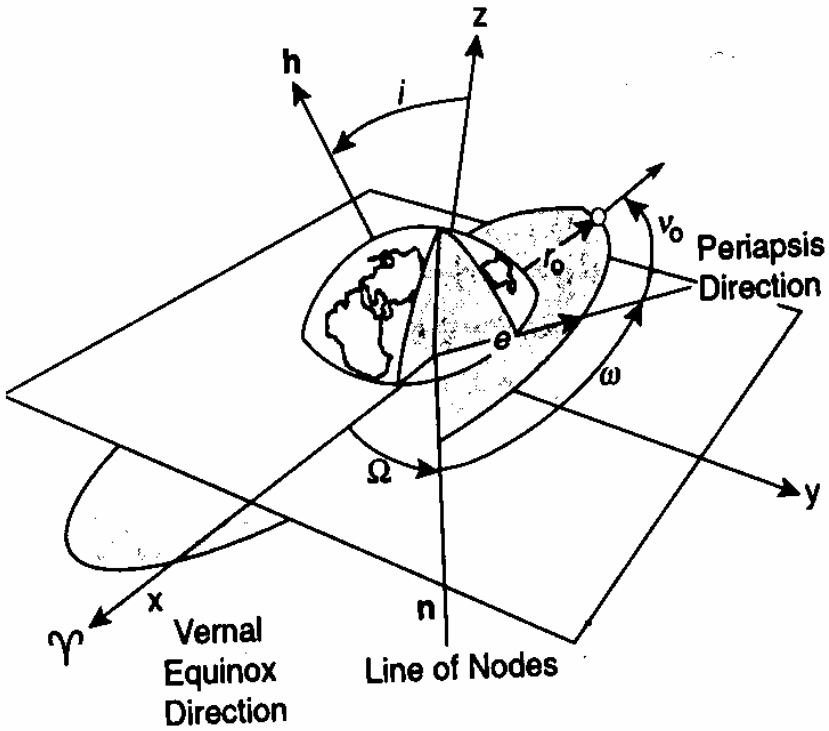
z
h
i
ν_o
Periapsis
Direction
r_o
e
ω
Ω
y
x
♈
Vernal
Equinox
Direction
n
Line of Nodes

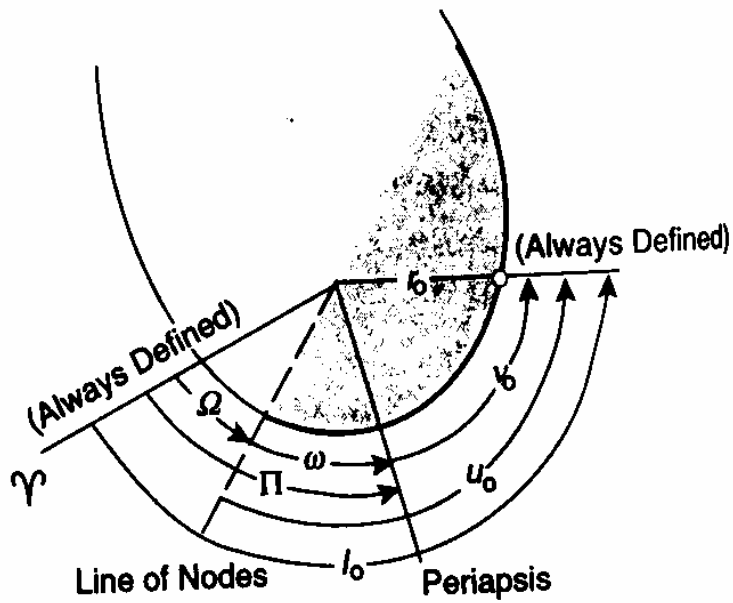
(Always Defined)
(Always Defined)
i_o
Ω
ω
Π
u_o
l_o
♈
Line of Nodes
Periapsis

6.1.3 Classical Orbital Elements

When solving the two-body equations of motion, we need six constants of integration (initial conditions) for the solution. Theoretically, we could find the three components of position and velocity at any time in terms of the position and velocity at any other time. Alternatively, we can completely describe the orbit with five constants and one quantity which varies with time. These quantities, called *classical orbital elements*, are defined below and are shown in Fig. 6-3. The coordinate frame shown in the figure is the geocentric inertial frame,* or GCI, defined in Chap. 5 (see Table 5-1). Its origin is at the center of the Earth, with the X-axis in the equatorial plane and pointing to the vernal equinox. Also, the Z-axis is parallel to the Earth's spin axis (the North Pole), and the Y-axis completes the right-hand set in the equatorial plane. The classical orbital elements are:

a: *semimajor axis*: describes the size of the ellipse (see Fig. 6-1).

e: *eccentricity*: describes the shape of the ellipse (see Fig. 6-1).

i: *inclination*: the angle between the angular momentum vector and the unit vector in the **Z**-direction.

Ω: *right ascension of the ascending node*: the angle from the vernal equinox to the ascending node. The *ascending node* is the point where the satellite passes through the equatorial plane moving from south to north. Right ascension is measured as a right-handed rotation about the pole, **Z**.

ω: *argument of perigee*: the angle from the ascending node to the eccentricity vector measured in the direction of the satellite's motion. The *eccentricity vector* points from the center of the Earth to perigee with a magnitude equal to the eccentricity of the orbit.

ν: *true anomaly*: the angle from the eccentricity vector to the satellite position vector, measured in the direction of satellite motion. Alternately, we could use *time since perigee passage*, T.

*A *sufficiently inertial coordinate frame* is a coordinate frame that we can consider to be non-accelerating for the particular application. The GCI frame is sufficiently inertial when considering Earth-orbiting satellites, but is inadequate for interplanetary travel because of its rotational acceleration around the Sun.

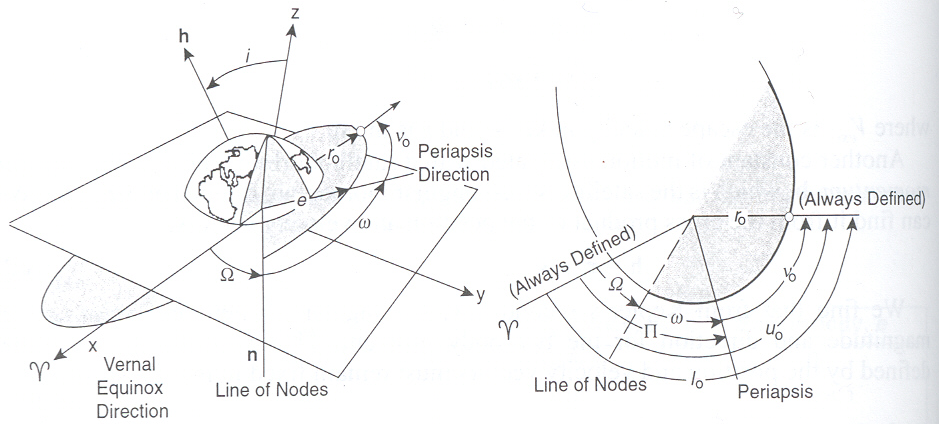

Fig. 6-3. Definition of the Keplerian Orbital Elements of a Satellite in an Elliptic Orbit. We define elements relative to the GCI coordinate frame.

4.4 ORBIT PERTURBATIONS

At the distances of orbiting spacecraft from the Earth its asphericity and non-uniform mass distribution result in its gravitational potential departing from the simple $1/r$ function, which was assumed in Section 4.2. Equation (4.1) is not valid in this situation and the equation of motion (4.4) must be modified to take account of the Earth's gravitational field.

There are additional forces that act on space vehicles, which were not included in the Keplerian formulation. Some are from additional masses that provide secondary gravitational fields; for Earth orbit, the Moon and the Sun provide such forces. Also, at low altitudes (typically at less than 1000 km altitude) the Earth's atmosphere imposes a drag force. Table 4.2 lists the major perturbing forces, and their relative importance, for space vehicle orbital analysis.

The equation of motion for a space vehicle about a body taking into account perturbative influences may be written in the form

$$\ddot{\mathbf{r}} = -\nabla U + \mathbf{b} \tag{4.33}$$

Table 4.2 Magnitude of disturbing accelerations acting on a space vehicle whose area-to-mass ratio is *A/M*. Note that A is the projected area perpendicular to the direction of motion for air drag, and perpendicular to the Sun for radiation pressure

Source	Acceleration (m/s^2)	
	500 km	Geostationary orbit
Air drag*	$6 \times 10^{-5} A/M$	$1.8 \times 10^{-13} A/M$
Radiation pressure	$4.7 \times 10^{-6} A/M$	$4.7 \times 10^{-6} A/M$
Sun (mean)	5.6×10^{-7}	3.5×10^{-6}
Moon (mean)	1.2×10^{-6}	7.3×10^{-6}
Jupiter (max.)	8.5×10^{-12}	5.2×10^{-11}

*Dependent on the level of solar activity

where U is the gravitational potential field and $\mathbf{b}$ is the force vector per unit mass due to other sources of perturbation, to which the vehicle is subject. A general closed solution is not possible, but there are a variety of solution methods that are appropriate for spacecraft dynamics. The 'variation of orbital elements' method is described here. Other methods such as those first proposed by Cowell and Crommelin [2] and Encke [3] are summarized by Cornelisse *et al.* [4].

The method of the variation of orbital elements may be considered in the following way. The elements referred to in the preceding section are constants for a Keplerian orbit, as derived in Section 4.2. When perturbative forces exist, they are no longer constant but for small forces they will change slowly.

A simple, physical model will serve to demonstrate this. Consider a spacecraft in circular orbit about a spherically symmetrical planet possessing an atmosphere of density ρ kg/m^3. If it is assumed that the perturbative drag force is small, then it is to be expected that the orbit will remain near circular. Now the velocity in a circular Keplerian orbit is given by $\sqrt{(\mu/r)}$. If the spacecraft's projected area in the direction of flight is S, then the work performed by the atmosphere as the vehicle moves round the orbit is given by $\sim -\pi r\rho S C_D \mu/r$, where C_D is an appropriate drag coefficient for the vehicle. Since this reduces the energy of the system, it is apparent that the energy constant ε in equation (4.21) will decrease and the orbital element a must do so too.

The variation of orbital elements method assumes that the actual orbit of a body, at any given instant, may be considered to have instantaneous values of Keplerian orbital elements. These are defined so that if the perturbing forces are removed at that instant, thus leaving only a central gravitational field whose potential is proportional to $1/r$, then the orbit will follow the Keplerian orbit that has the instantaneous orbital elements. These are called the *osculating elements*. It must be emphasized that the method is only appropriate for perturbing forces having a magnitude significantly smaller than μ/r^2.

The normal method for so describing an orbit is with recourse to Lagrange's planetary equations (see e.g. Reference [5]). One Gaussian form of these is the following [6]:

$$\left.\begin{aligned}
\frac{\mathrm{d}a}{\mathrm{d}\theta} &= \frac{2pr^2}{\mu(1-e^2)^2}\left\{e\sin\theta S + \frac{p}{r}T\right\}\\
\frac{\mathrm{d}e}{\mathrm{d}\theta} &= \frac{r^2}{\mu}\left\{\sin\theta S + \left(1+\frac{r}{p}\right)\cos\theta T + e\frac{r}{p}T\right\}\\
\frac{\mathrm{d}i}{\mathrm{d}\theta} &= \frac{r^3}{\mu p}\cos(\theta+\omega)W\\
\frac{\mathrm{d}\Omega}{\mathrm{d}\theta} &= \frac{r^3\sin(\theta+\omega)}{\mu p\sin i}W\\
\frac{\mathrm{d}\omega}{\mathrm{d}\theta} &= \frac{r^2}{\mu e}\left\{-\cos\theta S + \left(1+\frac{r}{p}\right)\sin\theta T\right\} - \cos i\frac{\mathrm{d}\Omega}{\mathrm{d}\theta}\\
\frac{\mathrm{d}t}{\mathrm{d}\theta} &= \frac{r^2}{\sqrt{(\mu p)}}\left\{1-\frac{r^2}{\mu e}[\cos\theta S - \left(1+\frac{r}{p}\right)\sin\theta T]\right\}
\end{aligned}\right\} \qquad (4.34)$$

where S, T, W form a triad of forces in a spacecraft-centred coordinate reference frame, S acting radially, T transverse to S in the orbital plane and directed positively in the sense of the spacecraft motion, and W normal to the orbit plane giving a right-handed system of forces. Strictly speaking, these components are those of the disturbing acceleration, though they are often referred to as components of the disturbing force.

4.4.1 Gravitational potential of the Earth

The most convenient method for describing Earth's gravitational field outside its surface is to use a spherical harmonic expansion [8], given by

$$U(r, \Phi, \Lambda) = \frac{\mu}{r}\left\{-1 + \sum_{n=2}^{\infty}\left[\left(\frac{R_E}{r}\right)^n J_n P_{n0}(\cos\Phi) + \sum_{m=1}^{n}\left(\frac{R_E}{r}\right)^n (C_{nm}\cos m\Lambda + S_{nm}\sin m\Lambda) P_{nm}(\cos\Phi)\right]\right\} \quad (4.35)$$

where $U(r, \Phi, \Lambda)$ is the gravitational potential at a distance r from the centre of the Earth and Φ, Λ are the latitude and longitude. P_{nm} are Legendre polynomials. J_n, C_{nm} and S_{nm} are dependent on the mass distribution of the body, in this case the Earth. Terms of the form J_n are called *zonal harmonic coefficients*; they reflect the mass distribution of the Earth independently of longitude. C_{nm} and S_{nm} are the Earth's *tesseral harmonic coefficients* for $n \neq m$ and the *sectoral harmonic coefficients* for $n = m$.

These coefficients have mainly been determined from the motion of Earth-orbiting spacecraft. Whilst the lower-order terms were determined during the early 1960s, determination of the Earth's gravitational field continues to be an area of active research. Consequently there is a plethora of 'standard' global gravity field models, for example, the Joint Gravity Model (JGM) series [9], of which the JGM-3 model is an example. This gives the harmonic coefficient values to degree and order 70.

One of the major problems in determination of the higher-order terms is due to their rapid decrease with altitude; from equation (4.35) terms decrease with $(R_E/r)^n$. However, at low altitudes there are also difficulties, since the gravity effects are difficult to separate from other perturbations, in particular, those due to variable air drag. This situation would be greatly improved by the launch of dedicated spacecraft missions to determine the higher-order harmonic coefficients in the Earth's gravity field. Promising proposals, such as the US GRAVSAT and the European ARISTOTELES missions, were stalled in the 1990s because of fiscal problems. However, with the launch of the CHAMP mission in July 2000, and that of other similar missions (e.g. GRACE) soon afterwards, the prospect of significantly improved gravitational field models has been enhanced.

Table 4.3 Magnitude of low-order *J*, *C* and *S* values for Earth

J_2	1082.6×10^{-6}	C_{21}	0	S_{21}	0
J_3	-2.53×10^{-6}	C_{22}	1.57×10^{-6}	S_{22}	-0.90×10^{-6}
J_4	-1.62×10^{-6}	C_{31}	2.19×10^{-6}	S_{31}	0.27×10^{-6}
J_5	-0.23×10^{-6}	C_{32}	0.31×10^{-6}	S_{32}	-0.21×10^{-6}
J_6	0.54×10^{-6}	C_{33}	0.10×10^{-6}	S_{33}	0.20×10^{-6}

Regression of the line of nodes

The equatorial bulge produces a torque that rotates the angular momentum vector. For prograde orbits ($i < 90°$), the orbit rotates in a westerly direction, leading to a regression of the line of nodes as shown pictorially in Figure 4.11. Neglecting all harmonic coefficients other than J_2, the rate of nodal regression may be written [7] to the first order in J_2 as

$$\overline{\Omega} = \Omega_0 - \frac{3}{2}\frac{J_2 R_E^2}{p^2}\overline{n}t\cos i + O[J_2^2] \tag{4.36}$$

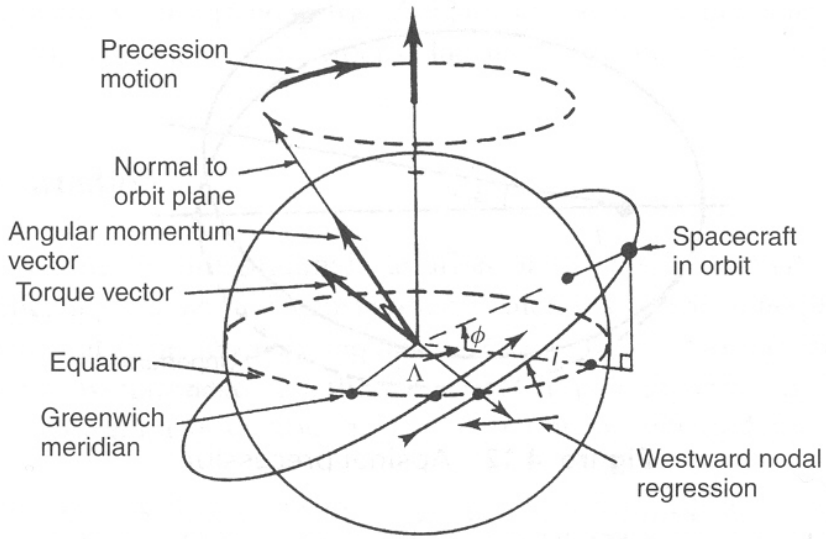

Figure 4.11 Nodal regression

where $\overline{n}$ is the mean angular velocity, $\sqrt{(\mu/a^3)}$. Thus, the secular rate of nodal regression per orbit is

$$\Delta\Omega = -\frac{3\pi J_2 R_E^2}{p^2}\cos i \text{ rad/rev} \tag{4.37}$$

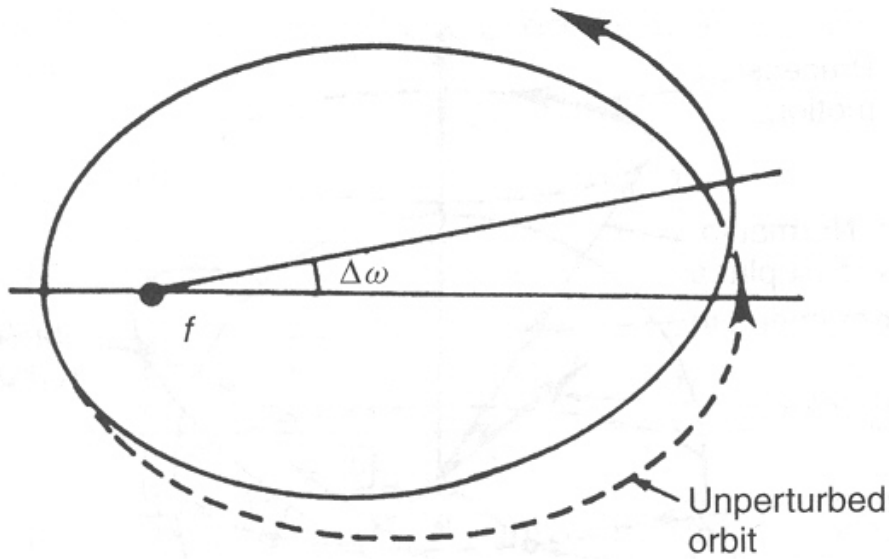

Figure 4.12 Apsidal precession

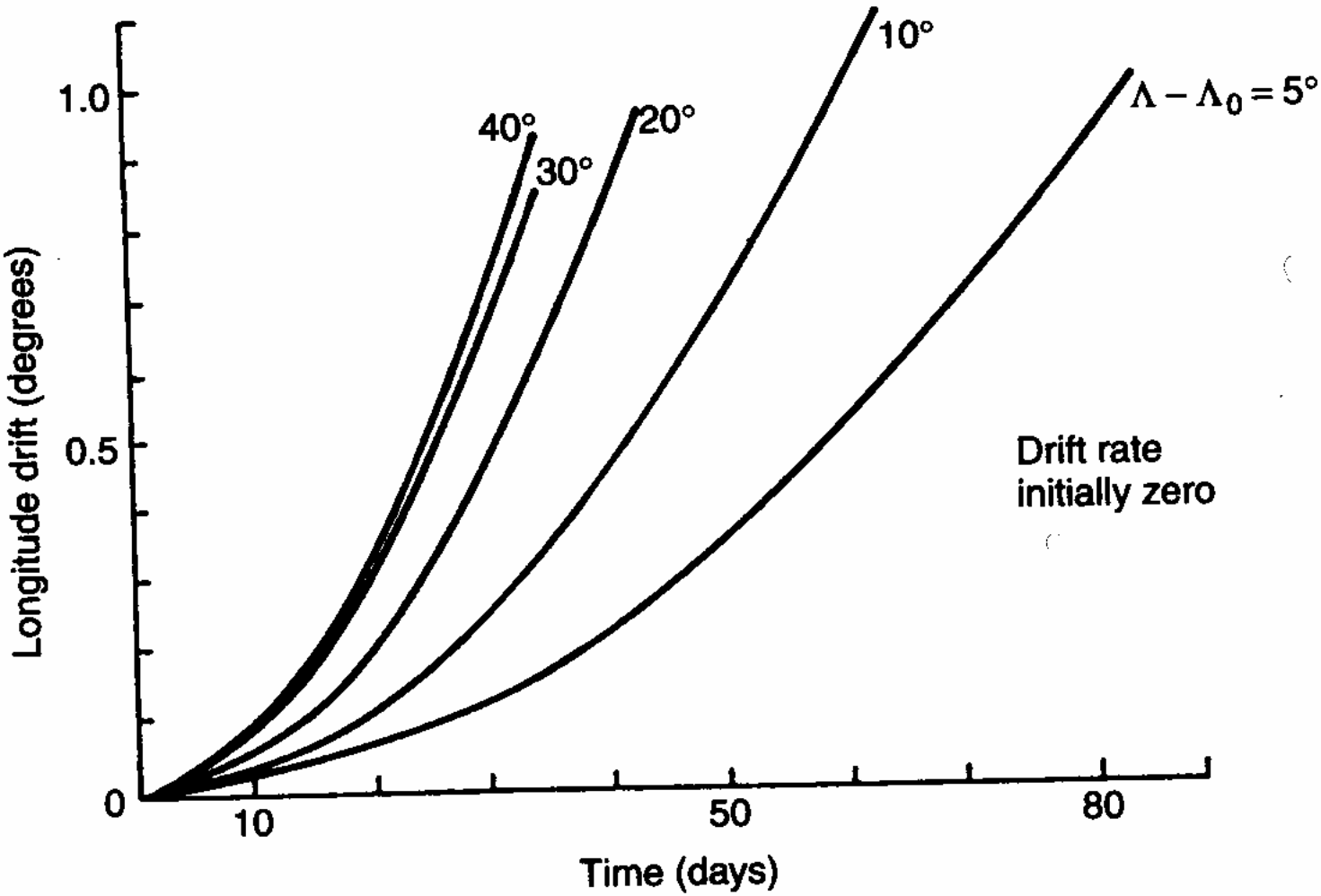

Figure 4.13 Longitudinal drift acquired over a period in geostationary orbit, as a function of the difference ($\Lambda - \Lambda_0$) in initial operating longitude and minor axis (stable) longitude

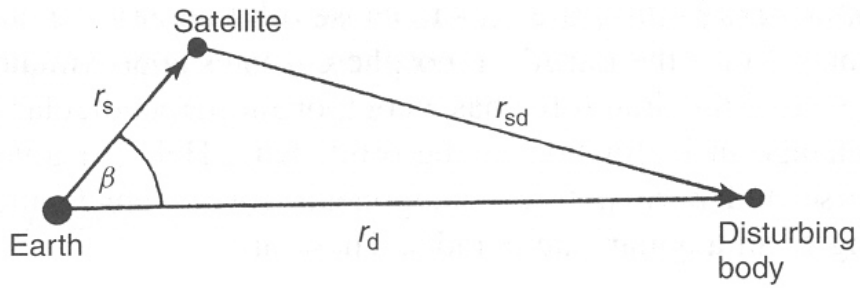

Figure 4.14 Disturbing body and satellite positions

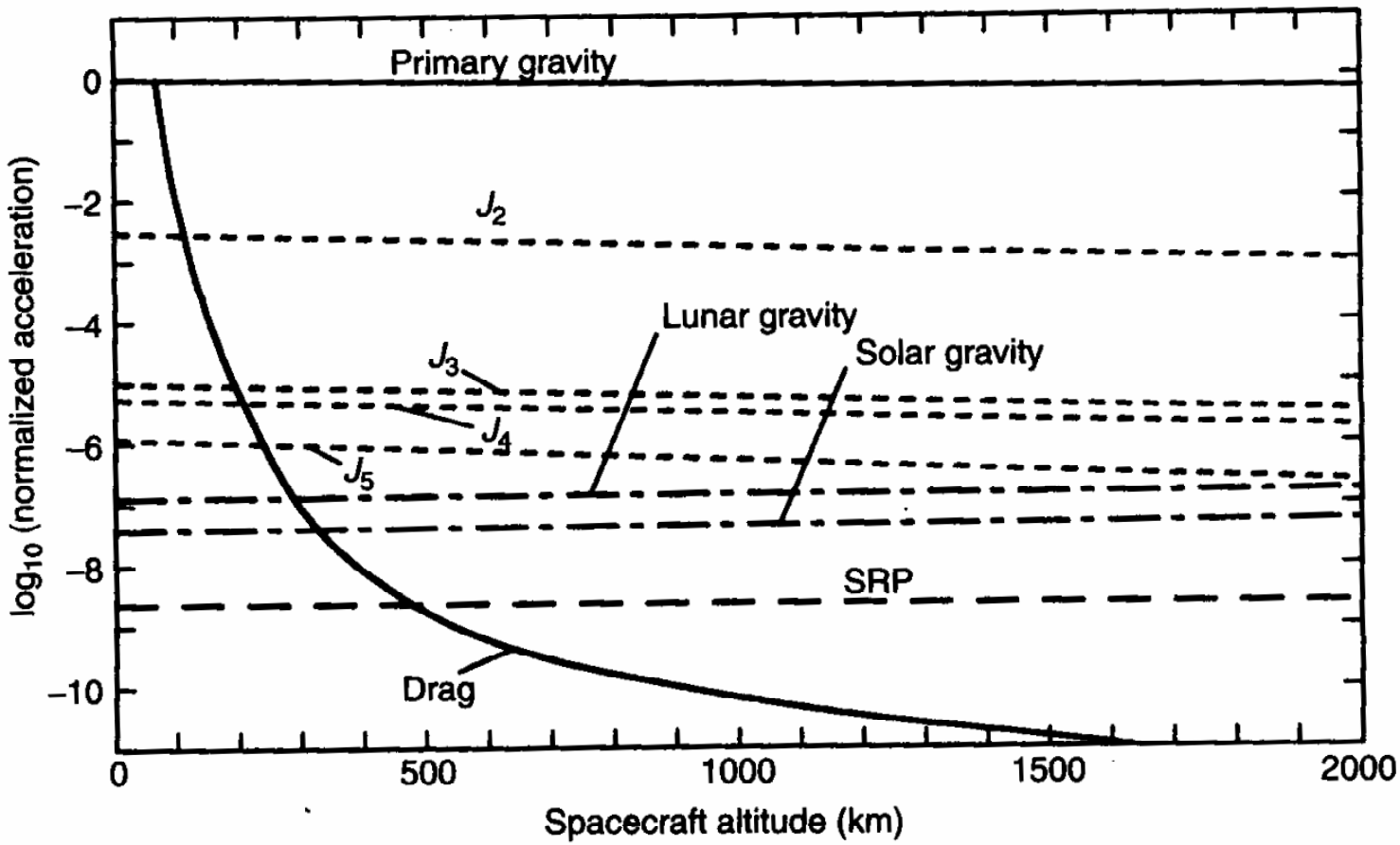

Figure 4.15 Comparisons of the disturbing accelerations for the main sources of perturbation

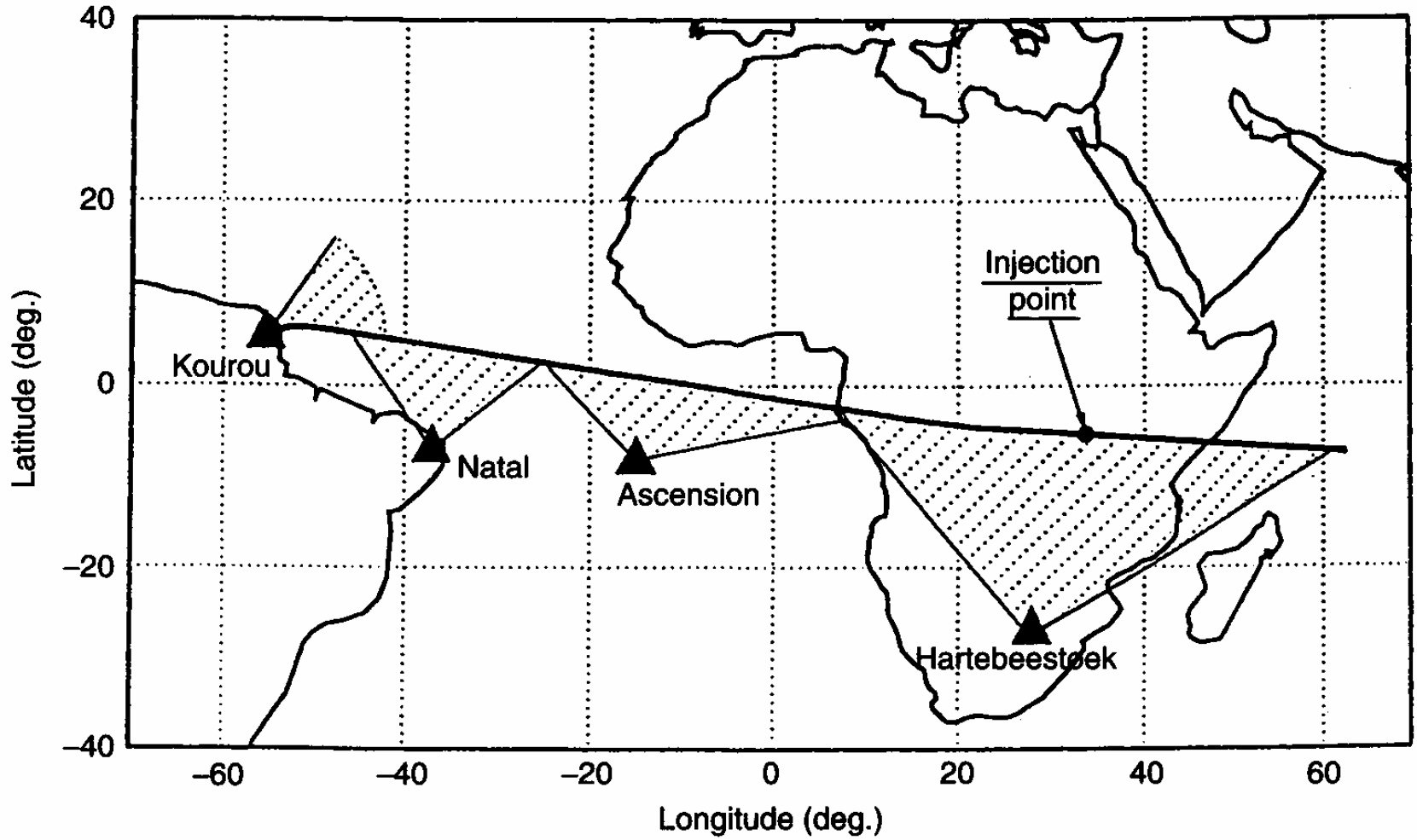

Figure 5.1 Typical Ariane 5 ground-track, showing launch monitoring ground stations (Reproduced by permission of Arianespace)

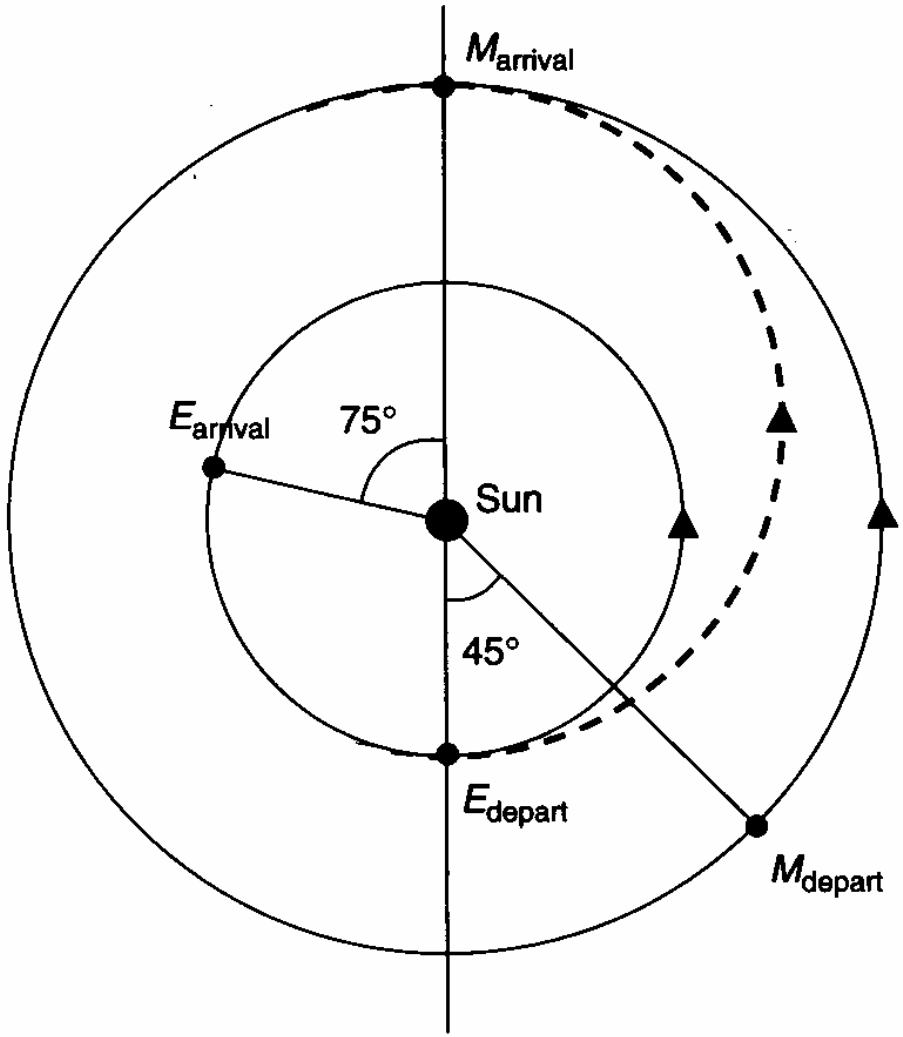

Figure 5.5 Planetary geometry at Earth departure and Mars arrival for a Hohmann transfer mission

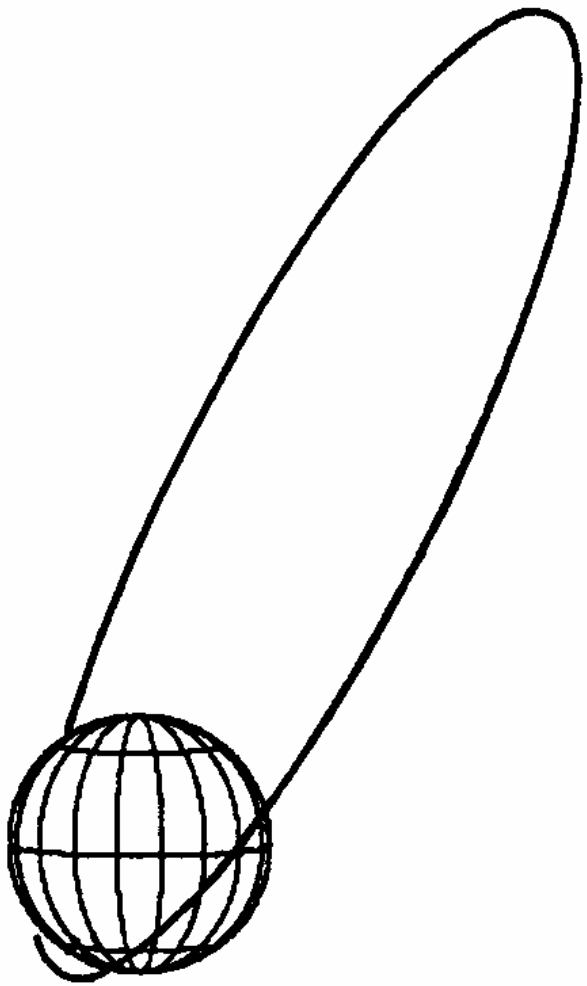

Figure 5.24 The Molniya orbit